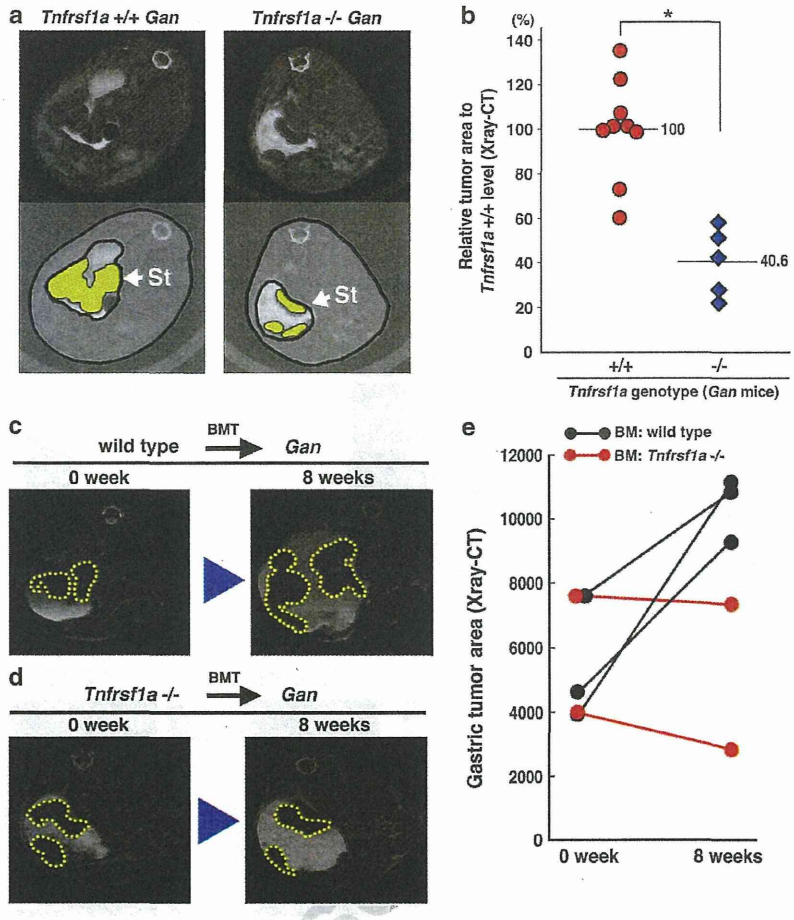

Figure 3. Suppression of gastric tumorigenesis by *Tnfrsf1a* disruption. (**a**) Representative X-ray CT slice images of *Tnfrsf1a* + / + *Gan* mice (left) and *Tnfrsf1a* − / − *Gan* mice (right). The stomach and tumor areas are indicated by lines and yellow color, respectively, in the copy CT images (bottom). (**b**) The calculated mean tumor area of *Tnfrsf1a* + / + *Gan* and *Tnfrsf1a* − / − *Gan* mice measured using slice images relative to the calculated mean tumor area of *Tnfrsf1a* + / + *Gan* mice (set at 100%). Asterisk (*), $P<0.05$. (**c**, **d**) Representative X-ray CT images of wild-type BM-transplanted *Gan* mice (**c**) and *Tnfrsf1a* − / − BM-transplanted *Gan* mice (**d**) at 0 weeks (left) and 8 weeks (right) after BM transplantation. The gastric tumor areas are indicated with yellow dashed lines. (**e**) The calculated mean tumor area from the X-ray CT slice images of wild-type BM-transplanted *Gan* mice (black line) and *Tnfrsf1a* − / − BM-transplanted *Gan* mice (red line) at 0 and 8 weeks after BM transplantation.

IκBα was increased in *Gan* mouse tumors compared with the wild-type mouse stomach (Figure 4a). In contrast, the IκBα phosphorylation level was significantly decreased in *Tnf* − / − *Gan* mouse tumors, indicating that NF-κB activation in tumors was suppressed by the disruption of *TNF-α* gene. On the other hand, the levels of phosphorylated Stat3 were increased significantly in both the *Tnf* + / + and *Tnf* − / − *Gan* mouse tumors to similar levels compared with the wild-type mouse level, suggesting that the cytokine pathways other than the TNF-α/NF-κB signaling were not suppressed in the *Tnf* − / − *Gan* mouse tumors.

Consistently, infiltration of T cells and macrophages were found in the *Tnf* − / − *Gan* mouse gastric tumors, similar to what they had in the *Tnf* + / + *Gan* mouse tumors (Figure 4b). The expression levels of IL-1β, IL-6, CXCL1 and CXCL2 in the gastric tumors were increased in the *Tnf* + / + *Gan* mouse tumors (Figure 4c). Notably, in the *Tnf* − / − *Gan* mouse tumors, the expression levels of these cytokines and chemokines significantly increased compared with those in wild-type mouse stomach, thus indicating that inflammation was not suppressed by *Tnf* gene disruption. It is therefore possible that the activation of TNF-α signaling is required for gastric tumor promotion, even if other tumor-promoting cytokines, such as IL-1β and IL-6, are induced in the tumor tissues.

Differentiation of tumor cells by *TNF-α* gene disruption

To identify the tumor-promoting factors that are induced by a TNF-α, we performed a microarray analysis using *Tnf* − / − *Gan* and *Tnf* + / + *Gan* mouse tumors and wild-type mouse stomachs (Gene Expression Omnibus (GEO) accession GSE43145). Using the microarray results, we extracted genes that were upregulated ⩾twofold in *Tnf* + / + *Gan* mouse tumors compared with wild-type mouse stomachs (Figure 5a). We next extracted the genes that were significantly downregulated in *Tnf* − / − *Gan* mouse tumors compared with *Tnf* + / + *Gan* mice. By comparing these two gene sets, 157 genes were identified that were upregulated in gastric tumors in a TNF-α-dependent manner (Figure 5b and Supplementary Table 1). Interestingly, *CD44*, *Prom1*, *Sox9* and *EphB3* were significantly donwregulated in *Tnf* − / − *Gan* mouse tumors, which are known markers of stem cells or progenitor cells in the intestine and liver,[24,25] suggesting that differentiation of tumor cells was induced by inhibition of TNF-α signaling.

We have previously demonstrated that expression of CD44 is induced in *Gan* mouse tumors.[26,27] Because CD44 is a marker of normal and cancer stem cells,[28] we examined CD44 expression and differentiation status of epithelial cells in *Tnf* − / − *Gan* mouse tumors. In the *Tnf* + / + or *Tnf* + / − *Gan* mouse tumors, CD44 mRNA levels increased significantly, by more than eightfold, the

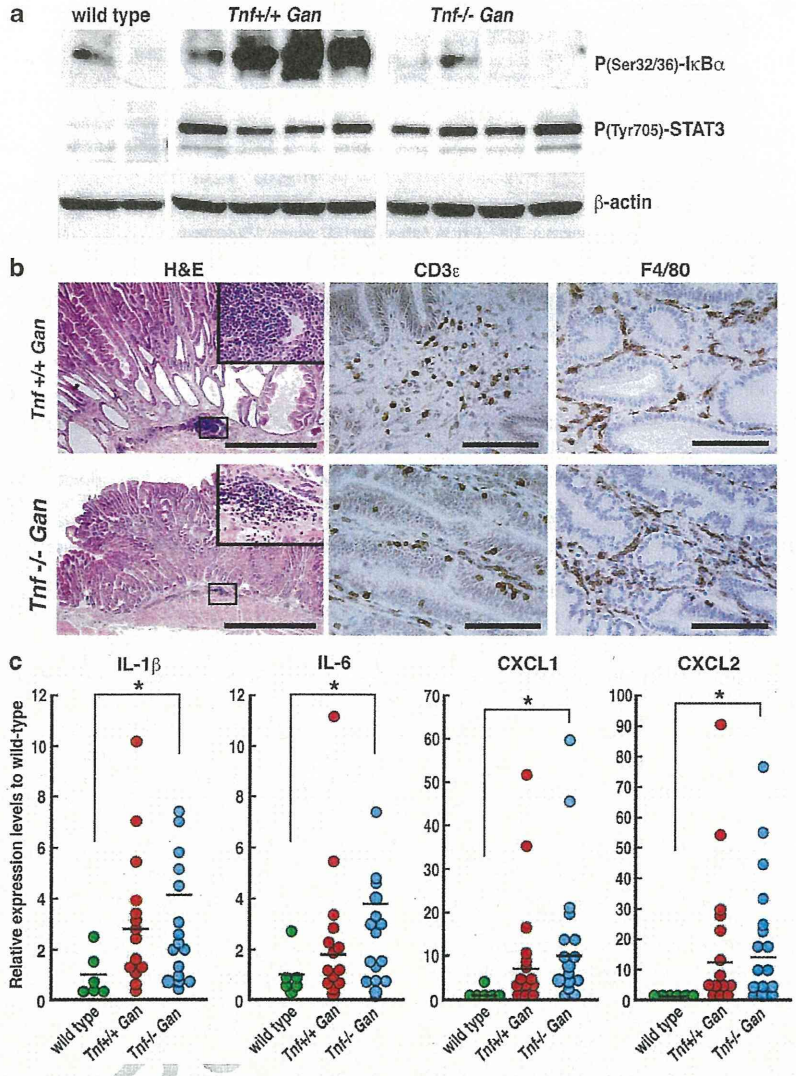

Figure 4. Inflammatory responses induced in *Tnf*−/− *Gan* mouse gastric tumors. (**a**) Immunoblotting of phosphorylated IκBα at Ser32/36 and phosphorylated Stat3 at Tyr705 in gastric tumors from *Tnf*+/+ *Gan* and *Tnf*−/− *Gan* mice ($n=4$ for each), as well as wild-type mouse normal stomach ($n=2$). β-Actin was used as an internal loading control. (**b**) Histological sections of *Tnf*+/+ *Gan* (top) and *Tnf*−/− *Gan* mouse tumors (bottom). H&E staining (left), immunostaining for a T cell marker, CD3ε (center) and a macrophage marker, F4/80 (right). The insets in the H&E staining images show submucosal mononuclear cell infiltration. Scale bars indicate 1 mm (left) and 100 μm (center/right). (**c**) The mRNA levels of the indicated cytokines and chemokines in the wild-type mouse stomach (green), gastric tumors of *Tnf*+/+ *Gan* (red) and *Tnf*−/− *Gan* (blue) mice relative to the mean level of a wild-type mouse stomach. Asterisks (*), $P<0.05$.

level observed in wild-type mice (Supplementary Figure 3a). In the *Tnf*−/− *Gan* mouse tumors, however, the CD44 induction was only about 4.5-fold than that of the wild-type stomachs. Notably, expression of differentiation markers, Muc5AC and H^+K^+/ATPase, was detected in the CD44-negative epithelial cells in *Tnf*−/− *Gan* mouse tumors, whereas CD44-positive tumor cells did not express these markers (Supplementary Figure 3b). Moreover, Ki-67-positive cells were predominantly found in the CD44-positive cell population. These results suggest that disruption of *TNF-α* gene causes differentiation of tumor epithelial cells, resulting in suppression of proliferation.

Candidate tumor-promoting factors induced by TNF-α

To select candidate genes whose products function to maintain the undifferentiated status, we compared the selected 157 genes with a gene set that was upregulated ⩾twofold in Lgr5+ gastric stem cells.[29] As a result, we found that 11 out of the 157 genes were upregulated also in gastric stem cells (Figure 5c). We next transfected small interfering RNAs (siRNAs) against these 11 genes into Kato-III cells, and examined the cell growth in soft agar. Notably, inhibition of *Noxo1*, *Gna14* and *Prom1* expression resulted in a significant decrease of cell proliferation in soft agar (Figure 6a). We further examined the tumorigenicity of Kato-III, MKN45 and MKN74 gastric cancer cells by transfection with siRNAs targeting different sequences of *Noxo1*, *Gna14*, and *Prom1*. Notably, siRNAs for *Noxo1* or *Gna14* suppressed the soft agar colony formation in all cell lines, while *Prom1* siRNAs suppressed only in Kato-III cells (Figure 6b and Supplementary Figure 4). Moreover, we found by reverse transcription-PCR (RT–PCR) that expression of *Noxo1* and *Gna14* was induced in gastric tumor epithelial cells as well as the tumor tissues of *Gan* mice (Figures 6c

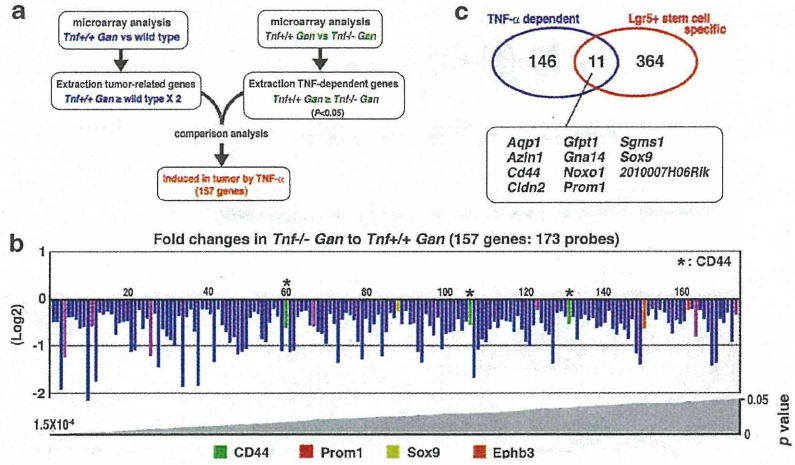

Figure 5. Extraction of candidate TNF-α-dependent tumor-promoting genes. (**a**) Strategy used for the selection of genes that were induced in gastric tumors in a TNF-α-dependent manner. (**b**) The fold-changes in the expression levels of the 157 TNF-α-dependent genes (173 probes) in *Tnf*−/− *Gan* mouse tumors compared with those in *Tnf*+/+ *Gan* mice (Log2 ratio). These genes were significantly downregulated in *Tnf*−/− *Gan* mouse tumors compared with *Tnf*+/+ *Gan* mouse tumors ($P<0.05$). Asterisks (*) indicate the three probes for CD44. Stem cell-related genes (CD44, Prom1, Sox9 and EphB3) are shown by bars with different colors. (**c**) A Venn diagram of 'induced genes in gastric tumors in a TNF-α-dependent manner (157 genes)' and 'upregulated genes ⩾twofold in Lgr5+ gastric stem cells (375 genes)'. Eleven genes were upregulated in both tumor tissues and Lgr5+ stem cells. These genes are indicated by bars in different colors in **b**.

and d). Accordingly, it is possible that TNF-α plays a tumor-promoting role through the induction of *Noxo1* and *Gna14* in tumor epithelial cells.

Role of Noxo1 and Gna14 in differentiation and cancer cell stemness

Differentiation of the primary cultured gastric epithelial cells was associated with the downregulation of a *Sox9* and induction of *Muc5AC* expression (Figure 6e). *Sox9* and *Muc5AC* are markers for undifferentiated and differentiated status, respectively. Notably, expression of both *Noxo1* and *Gna14* was decreased significantly in the differentiated epithelial cells compared with the undifferentiated cells, suggesting a role for Noxo1 and Gna14 in maintenance of undifferentiated status. We therefore examined the role of Noxo1 and Gna14 in the sphere formation of gastric cancer cells. MKN74 cells formed sphere colonies under hypoxic conditions, which were thought to reflect the characteristic of cancer stem cells. Notably, inhibition of *Noxo1* and *Gna14* expression by transfection of siRNAs resulted in a significant decrease in the number of sphere colonies, suggesting that Noxo1 and Gna14 have a role in maintaining the stemness of gastric cancer cells (Figures 6f and g).

TNF-α and CD44 in human gastric cancer tissues

Finally, we examined the expression of TNF-α and CD44 in human primary gastric cancers by real-time RT–PCR. The expression of TNF-α and CD44 was upregulated in 65% and 74% of gastric cancer tissues, respectively, and the expression of TNF-α and CD44 was positively correlated (Supplementary Figure 5). Therefore, it is possible that undifferentiated status of cancer cells is related to the level of TNF-α signaling also in the human gastric cancer.

DISCUSSION

Polymorphism of *TNF-α* gene is associated with an increased risk of gastric cancer, suggesting a role for TNF-α in gastric tumorigenesis.[7,9] In the present study, we have demonstrated, for the first time, that the induction of TNF-α signaling through TNFR1 promotes gastric tumorigenesis through inducing tumor-promoting factors, *Noxo1* and *Gna14*, in tumor epithelial cells (Figure 7).

One of the most important points of the present study is that we have successfully separated TNF-α signaling from COX-2/PGE_2-associated inflammatory responses in tumor tissues. Inflammatory cytokine signaling, including TNF-α, IL-6 and CXCL12, is induced simultaneously in tumor tissues, and the cytokine pathways activate each other by constructing a cytokine network.[30] Some of the inflammatory mediators have been shown to have a role in tumorigenesis. For example, we and other groups[31–33] have demonstrated that the COX-2/PGE_2 pathway has an essential role in gastrointestinal tumorigenesis by inducing angiogenesis and activation of Wnt signaling. Moreover, IL-6 and Stat3 are important for the development of colitis-associated colon cancer,[34,35] and constitutive activation of IL-1β signaling can induce gastric tumorigenesis.[10] It has also been reported that CXCL1/2 expression is linked to chemoresistance and metastasis.[36] Notably, the COX-2/PGE_2, IL-1β, IL-6 and CXCL1/2 pathways were still induced in the *Tnf*−/− *Gan* mouse tumors, possibly as a result of the transgenic expression of *Ptgs2* and *Ptges*. Accordingly, the present results clearly indicate that TNF-α signaling is required for gastric tumor development, even when an inflammatory network of other cytokines/chemokines is present.

It has been shown that the TNF-α receptor, TNFR1, signaling has a role in tumor development in chemically induced skin tumor and colitis-associated colon cancer mouse models.[16,17] In this study, we also showed that disruption of the *TNFR1* gene resulted in significant suppression of gastric tumorigenesis. Accordingly, it is possible that TNFR1 is the major receptor of TNF-α involved in gastric tumor promotion. In the present study, we found that TNF-α/TNFR1 signaling in BMDCs is important for gastric tumor growth. However, blocking TNFR1 signaling did not induce an effective regression of tumors even at 8 weeks after BM transplantation. It is possible that more than 8 weeks are required for established gastric tumors to regress by blocking the TNF/TNFR1 pathway. Moreover, TNFR1 is also expressed in the epithelial cells. Thus, it is conceivable that TNF-α signaling through TNFR1 on epithelial cells also contributes to gastric tumorigenesis, although it remains to be investigated.

Here, we have identified two tumor-promoting factors, Noxo1 and Gna14, which have a role in maintaining the tumorigenicity

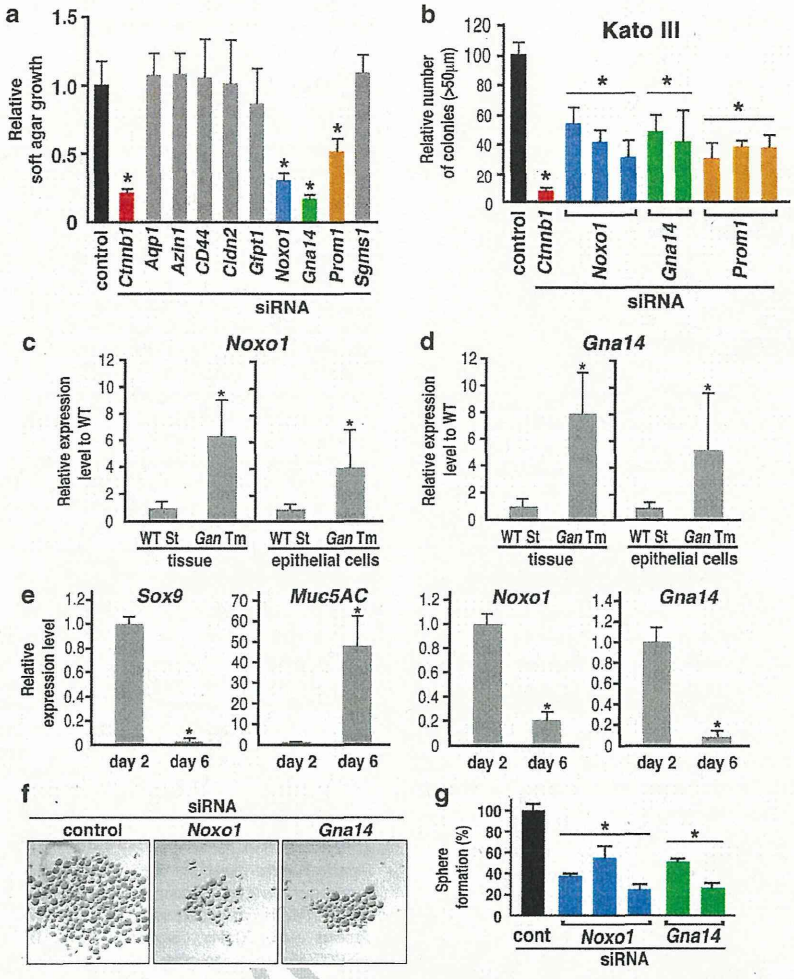

Figure 6. The roles of Noxo1 and Gna14 in tumorigenicity and stemness characteristics. (**a**) The cell growth in soft agar examined by fluorescence intensity of the indicated siRNA-transfected Kato-III cells relative to the mean value of control siRNA-transfected cells (mean ± s.d.). Asterisks (*), *P*-value <0.05 versus control. β-catenin gene (*Catnnb1*) siRNA was used as a positive control. (**b**) The numbers of soft agar colonies of the indicated siRNA-transfected Kato-III cells relative to the mean control siRNA level (mean ± s.d.). Individual bars in the same color indicate results of different siRNAs targeting different sequences for the same gene. Asterisks (*), *P*-value <0.05 versus control. (**c**, **d**) The mRNA levels of *Noxo1* (**c**) and *Gna14* (**d**) in tissues (left) or isolated epithelial cells (right) of wild-type (WT) mouse stomach (*WT St*) or *Gan* mouse tumors (*Gan Tm*) relative to the mean value of WT mouse level (mean ± s.d.). Asterisks (*), *P*-value <0.05 versus WT level. (**e**) The relative mRNA levels of the indicated genes in undifferentiated (day 2) or differentiated gastric epithelial cells (day 6; mean ± s.d.). Asterisks (*), *P*-value <0.05 versus the day 2 level. (**f**) Representative photographs of the spheres of control siRNA-transfected (left) and *Noxo1*- (center) or *Gna14*-siRNA-transfected (right) MKN74 cells. (**g**) The ratio of sphere formation by *Noxo1*- or *Gna14*-siRNA-transfected MKN74 cells relative to the mean level of control siRNA-transfected cells (mean ± s.d.). Individual bars in the same color indicate results of different siRNAs targeting different sequences for the same gene. Asterisks (*), *P*-value <0.05 versus control level.

and stemness of gastric cancer cells. It is possible that one of the tumor-promoting mechanisms of TNF-α signaling is the maintenance of the stemness of cancer cells. *Noxo1* encodes NOX-organizing protein 1, which is a component of the cytosolic regulatory subunits of NOX, and is associated with catalytic isoform NOX1.[37] NOX1 is one of the NOX family members, which are reactive oxygen species-generating enzymes that regulate the redox-sensitive signaling pathways. It has been reported that NOX1 expression is upregulated by oncogenic Ras activation and is required for transformation of cancer cells.[38,39] Moreover, a microarray analysis indicated that *Noxo1* expression is upregulated in a subpopulation of colon cancers.[40] Accordingly, it is possible that *Noxo1* is induced in cancer cells, together with NOX1, in the inflammatory microenvironment, contributing to an oncogene-induced transformation phenotype through the generation of reactive oxygen species.

In contrast to NOX1, little is known about the role(s) of Gna14 in tumor development. *Gna14* encodes guanine nucleotide-binding protein subunit alpha14 ($G\alpha_{14}$), a member of the $G_q\alpha$ subfamily of G proteins.[41] $G\alpha_{14}$ is employed by a variety of G protein-coupled receptors, including somatostatin type 2 receptor and chemokine receptor CCR1, which activate the NF-κB pathway.[42,43] Recently, it has been reported that activation of NF-κB in the Wnt-activated cells induces dedifferentiation in intestinal epithelial cells, resulting in the acquisition of tumor-initiating property.[44] Accordingly, it is possible that *Gna14* expression contributes to maintaining tumor cells in an undifferentiated status through activation of NF-κB, which leads to tumor development.

Noxo1 and *Gna14* were induced in the tumor epithelial cells, whereas TNF-α/TNFR1 signaling was predominantly activated in the BMDCs of *Gan* mouse tumors. Accordingly, it is possible that the expression of *Noxo1* and *Gna14* in tumor cells is not directly

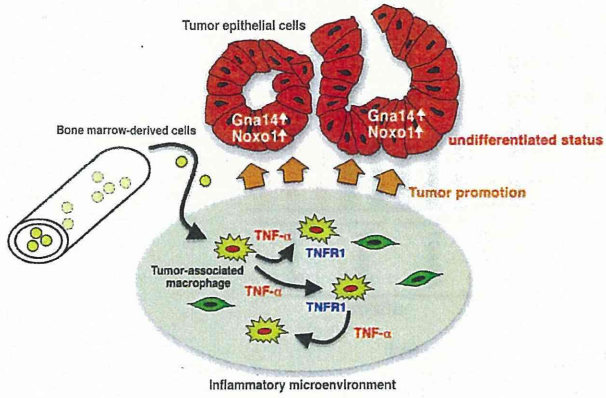

Figure 7. A schematic drawing of the role of TNF-α signaling in gastric tumorigenesis. BMDCs, including macrophages, are recruited to the inflammatory microenvironment and express TNF-α, which further activates TNFR1 receptor on BMDCs in the microenvironment, which is important for inducing the tumor-promoting factors including *Noxo1* and *Gna14* in tumor epithelial cells.

regulated by TNF-α signaling, but indirectly through BMDC-expressing molecule(s) that are induced by the TNF-α/NF-κB pathway. It is therefore conceivable that such a molecule would be an effective target for the prevention or treatment of gastric cancer.

In conclusion, we demonstrated that TNF-α/TNFR1 signaling in the tumor microenvironment promotes gastric cancer development. *Noxo1* and *Gna14* are induced in tumor epithelial cells by a TNF-α-dependent manner, which is important for gastric tumorigenesis. Accordingly, it is possible that targeting TNF-α signaling in the microenvironment, or inhibition of Noxo1 and Gna14 induction or their functions in tumor cells, may represent a preventive or therapeutic strategy against gastric cancer.

MATERIALS AND METHODS

Animal models

K19-Wnt1 mice express *Wnt1* driven by the *Krt19* gene promoter, which is transcriptionally active in gastric epithelial cells, whereas *Gan* mice express *Wnt1*, *Ptgs2* and *Ptges*, driven by the *Krt19* promoter.[18,19] *Tnf* mutant mice were purchased from Jackson Laboratories (Bar Harbor, ME, USA), and *Tnfrsf1a* mutant mice were described previously.[17] For the tumor phenotype analyses, *Gan* mice were euthanized and examined at 50 weeks of age ($n=8$ for *Tnf*+/+ *Gan* mice and *Tnf*−/− *Gan* mice, and $n=10$ for *Tnf*+/− *Gan* mice) or examined by a X-rayCT analysis at 25 weeks of age ($n=9$ for *Tnfrsfr1a*+/+ *Gan* mice, and $n=5$ for *Tnfrsf1a*−/− *Gan* mice). All animal experiments were carried out according to the protocol approved by the Committee on Animal Experimentation of Kanazawa University, Japan.

Measurement of tumor volume and scoring of preneoplastic lesions

The tumor area was measured by the ImageJ 1.46 software program (NIH, Bethesda, MD, USA) using photographs that were taken under a dissecting microscope. The mucosal thickness (tumor height) of the gastric tumors was measured using histology sections. The 'tumor size' was calculated by multiplying the tumor area by the tumor height ('tumor area' × 'tumor height'). The relative tumor size was calculated in comparison with the mean of the control *Gan* mouse tumor size. The X-ray CT images of the gastric tumors were examined using a LaTheta LCT-100 instrument (Aloka, Tokyo, Japan). The tumor areas of the slice images were measured using the ImageJ 1.46 software program (NIH), and three serial images, including the largest tumor image, were selected from all scanned images for each mouse, and the mean tumor area of the three images was calculated and compared with the mean value of the control *Gan* mice. The number of preneoplastic lesions in the glandular stomachs of *K19-Wnt1* mice ($n=6$ for each genotype) was counted using eight independent histology sections, and the mean number per section was calculated.

Real-time RT-PCR

Gastric tumors of *Tnf*+/+ *Gan* ($n=7$) and *Tnf*−/− *Gan* mice ($n=8$), and normal stomachs of wild-type mice ($n=6$), were used for RNA extraction. For human tissue samples, paired samples of human gastric cancer tissues and adjacent normal stomach tissues ($n=23$) were collected at Kanazawa University Hospital, Japan. For experiments using human tissue samples, approval for the project was obtained from the Kanazawa University Medical Ethics Committee, and written informed consent was obtained before specimen collection. The total RNAs of tissue samples were extracted using ISOGEN (Nippon Gene, Tokyo, Japan), reverse-transcribed using the PrimeScript RT reagent kit (Takara, Tokyo, Japan) and were PCR-amplified by a Stratagene Mx3000P instrument (Agilent Technologies, Santa Clara, CA, USA) using SYBR Premix ExTaqII (Takara). To avoid location-related differences in the differentiation and proliferation status within a *Gan* mouse tumor tissue, two samples were collected from different regions of the same tumors. The primers used for the real-time RT–PCR were purchased from Takara. For laser microdissection-based RT–PCR, epithelial cells and stromal cells were separately collected from frozen sections of *Gan* mouse tumors ($n=4$) using laser microdissection LMD7000 (Leica Microsystems, Wetzler, Germany), and the total RNAs were extracted using a RNeasy Micro kit (Qiagen, Valencia, CA, USA).

BM transplantation

BM cells were prepared from the femurs and tibias of donor mice. Recipient mice were irradiated with 9 Gy, followed by intravenous injection of 2×10^6 BM cells. *Tnf*+/+ GFP mouse BM was transplanted into *Tnf*−/− *Gan* mice and *Tnf*−/− mice BM was transplanted into *Tnf*−/− *Gan* mice as a control. *Tnfrsf1a*−/− BM was transplanted into *Tnfrsf1a*+/+ *Gan* mice and wild-type mouse BM was transplanted into *Tnfrsf1a*+/+ *Gan* mice as a control. The X-ray CT images of the gastric tumors were examined at 0 and 8 weeks after BM transplantation.

Histology and immunohistochemistry

Tissues were fixed in 4% paraformaldehyde, paraffin-embedded and sectioned at 4 μm thickness. Sections were stained with hematoxylin and eosin (H&E) or processed for the immunohistochemistry. Antibodies against Ki-67 (Dako, Carpinteria, CA, USA), F4/80 (Serotec, Oxford, UK), GFP (Life Technologies, Grand Island, NY, USA), E-cadherin (R&D, Minneapolis, MN, USA), CD3ε (Santa Cruz Biotechnology, Santa Cruz, CA, USA), CD44 (Millipore, Billerica, MA, USA), Muc5AC (Thermo Fisher Scientific, Rockford, IL, USA) and H^+K^+/ATPase (MBL, Nagoya, Japan) were used as the primary antibodies. Staining signals were visualized using the Vectastain Elite Kit (Vector Laboratories, Burlingame, CA, USA). For fluorescence immunohistochemistry, Alexa Fluor 594 or Alexa Fluor 488 antibodies (Molecular Probes, Eugene, OR, USA) were used as the secondary antibody. One milliliter of BrdU was injected intraperitoneally (1 mg/ml; Roche Diagnostics, Indianapolis, IN, USA) 1.5 h before euthanasia, and tissue sections were immunostained with an anti-BrdU antibody (Roche).

Immunoblotting analysis

Tissues were homogenized in lysis buffer, and 10 μg of the supernatant protein sample was separated in a 10% SDS-polyacrylamide gel. Antibodies against phosphorylated IκBα at Ser32/36 and phosphorylated Stat3 at Tyr705 (Cell Signaling, Danvers, MA) were used. An anti-β-actin antibody (Sigma, St Louis, MO, USA) was used as the internal loading control. The ECL detection system (GE Healthcare, Buckinghamshire, UK) was used to detect the signals.

Microarray analysis

Total RNA was extracted from the gastric tumors of *Tnf*+/+ *Gan* mice and *Tnf*−/− *Gan* mice and wild-type mouse stomachs ($n=3$ for each) using ISOGEN (Nippon Gene). GeneChip Mouse Genome 430 2.0 Arrays (Affymetrix, Santa Clara, CA, USA) were used for the expression profile analyses. The labeled cRNA was prepared using standard Affymetrix protocols, and the chips were scanned using a GeneChip Scanner 3000 7G (Affymetrix). The microarray results were deposited in the GEO as accession GSE43145.

Cell culture experiments

Gastric cancer cell lines, MKN45, MKN74 and Kato-III (Riken Bioresource Center, Tsukuba, Japan) were cultured in RPMI1640 or DMEM supplemented with 10% fetal bovine serum. Knockdown experiments were performed using Silencer Select Pre-designed siRNA and negative control siRNA (Life Technologies, Carlsbad, CA, USA). For the soft agar proliferation/colony formation assay, cells were mixed in 0.4% agar and seeded in a 96-well or six-well plate and cultured for 1 or 3 weeks, respectively. Then, 96-well plates were stained with AlamarBlue reagent (Life Technologies), and the fluorescence intensity was measured to examine the cell number. Six-well plates were stained with Giemsa solution (Wako, Osaka, Japan) and colony numbers were scored. For the sphere formation assay, MKN74 cells were plated in ultra-low attachment plates (Corning, Corning, NY, USA) and were cultured under hypoxic conditions at 3% O_2 and 5% CO_2. After 10 days, the number of spheres was counted.

The primary culture of gastric epithelial cells was described previously.[45] Briefly, mouse glandular stomachs were treated with 0.1% collagenase, followed by centrifugation at 20 *g* for 3 min to isolate gastric glands. Isolated glands were digested with trypsin and cultured on collagen-coated dishes. On day 2, the cells were passaged to induce differentiation. The primary cultured cells on day 2 and day 6 were used as undifferentiated and differentiated gastric epithelial cells, respectively.

Statistical analysis

The data were analyzed using the unpaired *t*-test and are presented as the means ± s.d. A value of $P<0.05$ was considered to be statistically significant.

CONFLICT OF INTEREST

The authors declare no conflict of interest.

ACKNOWLEDGEMENTS

We thank Manami Watanabe and Ayako Tsuda for their excellent technical assistance. This work was supported by Grants-in-Aid for Scientific Research on Innovative Areas (no. 22114005) from the Ministry of Education, Culture, Sports, Science and Technology of Japan; and CREST, the Japan Science and Technology Agency, Japan.

REFERENCES

1 Parkin DM, Bray F, Ferlay J, Pisani P. Global cancer statistics, 2002. *CA Cancer J Clin* 2005; **55**: 74–108.
2 Peek Jr RM, Blaser MJ. *Helicobacter pylori* and gastrointestinal tract adenocarcinomas. *Nat Rev Cancer* 2002; **2**: 28–37.
3 Fox JG, Wang TC. Inflammation, atrophy, and gastric cancer. *J Clin Invest* 2007; **117**: 60–69.
4 Coussens LM, Werb Z. Inflammation and cancer. *Nature* 2002; **420**: 860–867.
5 Grivennikov SI, Greten FR, Karin M. Immunity, inflammation, and cancer. *Cell* 2010; **140**: 883–899.
6 El-Omar EM, Carrington M, Chow W-H, McColl KE, Bream JH, Young HA *et al.* Interleukin-1 polymorphisms associated with increased risk of gastric cancer. *Nature* 2000; **404**: 398–402.
7 EL-Omar EM, Rabkin CS, Gammon MD, Vaughan TL, Risch HA, Schoenberg JB *et al.* Increased risk of noncardia gastric cancer associated with proinflammatory cytokine gene polymorphisms. *Gastroenterology* 2003; **124**: 1193–1201.
8 Mochado JC, Figueiredo C, Canedo P, Pharoah P, Carvalho R, Nabais S *et al.* A proinflammatory genetic profile increases the risk for chronic atrophic gastritis and gastric carcinoma. *Gastroenterology* 2003; **125**: 364–371.
9 El-Omar EM. Role of host genes in sporadic gastric cancer. *Best Pract Res Clin Gastroenterology* 2006; **20**: 675–686.
10 Tu S, Bhagat G, Cui G, Takaishi S, Kurt-Jones EA *et al.* Overexpression of interleukin-1β induces gastric inflammation and cancer mobilizes myeloid-derived suppressor cells in mice. *Cancer Cell* 2008; **14**: 408–419.
11 Tebbutt NC, Giraud AS, Inglese M, Jenkins B, Waring P, Clay FJ *et al.* Reciprocal regulation of gastrointestinal homeostasis by SHP2 and STAT-mediated trefoil gene activation in gp130 mutant mice. *Nat Med* 2002; **8**: 1089–1097.
12 Tye H, Kennedy CL, Najdovska M, McLeod L, McCormack W, Hughes N *et al.* STAT3-driven upregulation of TLR2 promotes gastric tumorigenesis independent of tumor inflammation. *Cancer Cell* 2012; **22**: 466–478.
13 Balkwill F. TNF-α in promotion and progression of cancer. *Cancer Metastasis Rev* 2006; **25**: 409–416.
14 Balkwill F. Tumor necrosis factor and cancer. *Nat Rev Cancer* 2009; **9**: 361–371.
15 Moore RJ, Owens DM, Stamp G, Arnott C, Burke F, East N *et al.* Mice deficient in tumor necrosis factor-α are resistant to skin carcinogenesis. *Nat Med* 1999; **5**: 828–831.
16 Arnott CH, Scott KA, Moore RJ, Robinson SC, Thompson RG, Balkwill FR. Expression of both TNF-α receptor subtypes is essential for optimal skin tumour development. *Oncogene* 2004; **23**: 1902–1910.
17 Popivanova BK, Kitamura K, Wu Y, Kondo T, Kagaya T, Kanoko S *et al.* Blocking TNF-α in mice reduces colorectal carcinogenesis associated with chronic colitis. *J Clin Invest* 2008; **118**: 560–570.
18 Oshima H, Matsunaga A, Fujimura T, Tsukamoto T, Taketo MM, Oshima M. Carcinogenesis in mouse stomach by simultaneous activation of the Wnt signaling and prostaglandin E_2 pathway. *Gastroenterology* 2006; **131**: 1086–1095.
19 Oshima H, Oguma K, Du YC, Oshima M. Prostaglandin E_2, Wnt and BMP in gastric tumor mouse models. *Cancer Sci* 2009; **100**: 1779–1785.
20 Clements WM, Wang J, Sarnaik A, Kim OJ, MacDonald J, Fenoglio-Preiser C *et al.* *β-Catenin* mutation is a frequent cause of Wnt pathway activation in gastric cancer. *Cancer Res* 2002; **62**: 3503–3506.
21 Wang D, DuBois RN. Eicosanoids and cancer. *Nat Rev Cancer* 2010; **10**: 181–193.
22 Itadani H, Oshima H, Oshima M, Kotani H. Mouse gastric tumor models with prostaglandin E_2 pathway activation show similar gene expression profiles to intestinal-type human gastric cancer. *BMC Genomics* 2009; **10**: 615.
23 Oshima H, Hioki K, Popivanova BK, Oguma K, van Rooijen N, Ishikawa TO *et al.* Prostaglandin E_2 signaling and bacterial infection recruit tumor-promoting macrophages to mouse gastric tumors. *Gastroenterology* 2011; **140**: 596–607.
24 Itzkovitz S, Lyubimova A, Blat IC, Maynard M, van Es J, Lees J *et al.* Single-molecule transcript counting of stem-cell markers in the mouse intestine. *Nat Cell Biol* 2012; **14**: 106–114.
25 Huch M, Dorrell C, Boj SF, van Es JH, Li VS, van de Watering M *et al.* *In vitro* expansion of single $Lgr5^+$ liver stem cells induced by Wnt-driven regeneration. *Nature* 2013; **494**: 247–250.
26 Ishimoto T, Oshima H, Oshima M, Kai K, Torii R, Masuko T *et al.* $CD44^+$ slow-cycling tumor cell expansion is triggered by cooperative actions of Wnt and prostaglandin E_2 in gastric tumorigenesis. *Cancer Sci* 2010; **101**: 673–678.
27 Ishimoto T, Nagano O, Yae T, Tamada M, Motohara T, Oshima H *et al.* CD44 variant regulates redox status in cancer cells by stabilizing the xCT subunit of system xc(-) and thereby promotes tumor growth. *Cancer Cell* 2011; **19**: 387–400.
28 Zöller M. CD44: can a cancer-initiating cell profit from an abundantly expressed molecule? *Nat Rev Cancer* 2011; **11**: 254–267.
29 Barker N, Huch M, Kujala P, van de Wetering M, Snippert HJ, van Es JH *et al.* $Lgr5^{+ve}$ stem cells drive self-renewal in the stomach and build long-lived gastric units in vitro. *Cell Stem Cell* 2011; **6**: 25–36.
30 Kulbe H, Chakravarty P, Leinster DA, Charles KA, Kwong J, Thompson RG *et al.* A dynamic inflammatory cytokine network in the human ovarian cancer microenvironment. *Cancer Res* 2012; **71**: 66–75.
31 Seno H, Oshima M, Ishikawa TO, Oshima H, Takaku K, Chiba T *et al.* Cyclooxygenase 2-and prostaglandin E_2 receptor EP_2-dependent angiogenesis in $Apc^{\Delta 716}$ mouse intestinal polyps. *Cancer Res* 2002; **62**: 506–511.
32 Castellone MD, Teramoto H, Williams BO, Druey KM, Gutkind JS. Prostaglandin E_2 promotes colon cancer cell growth through a Gs-axin-β-catenin signaling axis. *Science* 2005; **310**: 1504–1510.
33 Oguma K, Oshima H, Aoki M, Uchio R, Naka K, Nakamura S *et al.* Activated macrophages promote Wnt signalling through tumour necrosis factor-αin gastric tumour cells. *EMBO J* 2008; **27**: 1671–1681.
34 Bollrath J, Phesse TJ, von Burstin VA, Putoczki T, Bennecke M, Bateman T *et al.* gp130-mediated Stat3 activation in enterocytes regulates cell survival and cell-cycle progression during colitis-associated tumorigenesis. *Cancer Cell* 2009; **15**: 91–102.
35 Grivennikov S, Karin E, Terzic J, Mucida D, Yu G-Y, Vallabhapurapu S *et al.* IL-6 and Stat3 are required for survival of intestinal epithelial cells and development of colitis-associated cancer. *Cancer Cell* 2009; **15**: 103–113.
36 Acharyya S, Oskarsson T, Vanharanta S, Malladi S, Kim J, Morris PG *et al.* A CXCL1 paracrine network links cancer chemoresistance and metastasis. *Cell* 2012; **150**: 165–178.
37 Block D, Gorin Y. Aiding and abetting roles of NOX oxidases in cellular transformation. *Nat Rev Cancer* 2012; **12**: 627–637.
38 Mitsushita J, Lambeth JD, Kamata T. The superoxide-generating oxidase Nox1 is functionally required for Ras oncogene transformation. *Cancer Res* 2004; **64**: 3580–3585.
39 Adachi Y, Shibai Y, Mitsushita J, Shang WH, Hirose K, Kamata T. Oncogenic Ras upregulates NADPH oxidase 1 gene expression through MEK-ERK-dependent phosphorylation of GATA-6. *Oncogene* 2008; **27**: 4921–4932.

40 Juhasz A, Ge Y, Markel S, Chiu A, Matsumoto L, van Balgooy J *et al.* Expression of NADPH oxidase homologues and accessory genes in human cancer cell lines, tumours and adjacent normal tissues. *Free Radic Res* 2009; **43**: 523–532.
41 Kostenis E, Waelbroeck M, Milligan G. Techniques: Promiscous Gα proteins in basic research and drug discovery. *TrendsPham Sci* 2005; **26**: 595–602.
42 Liu AMF, Wong YH. Activation of nuclear factor κB by somatostatin type 2 receptor in pancreatic acinar AR42J cells involves $G\alpha_{14}$ and multiple signaling components. *J Biol Chem* 2005; **280**: 34617–34625.
43 Lee MMK, Wong YH. CCR1-mediated activation of nuclear factor-κB in THP-1 monocytic cells involves *pertussis* toxin-insensitive $G\alpha_{14}$ and $G\alpha_{16}$ signaling cascade. *J Leukoc Biol* 2009; **86**: 1319–1329.
44 Schwitalla S, Fingerle AA, Cammareri P, Nebelsiek T, Göktuna SI, Ziegler PK *et al.* Intestinal tumorigenesis initiated by dedifferentiation and acquisition of stem-cell-like properties. *Cell* 2013; **152**: 25–38.
45 Kong D, Piao Y-S, Yamashita S, Oshima H, Oguma K, Fushida S *et al.* Inflammation-induced repression of tumor suppressor miR-7 in gastric tumor cells. *Oncogene* 2012; **31**: 3949–3960.

Supplementary Information accompanies this paper on the Oncogene website (http://www.nature.com/onc)

Biochemical Pharmacology xxx (2014) xxx–xxx

Contents lists available at ScienceDirect

Biochemical Pharmacology

journal homepage: www.elsevier.com/locate/biochempharm

DIF-1 inhibits tumor growth *in vivo* reducing phosphorylation of GSK-3β and expressions of cyclin D1 and TCF7L2 in cancer model mice

Fumi Takahashi-Yanaga [a,b,*], Tatsuya Yoshihara [a], Kentaro Jingushi [a], Kazuhiro Igawa [c], Katsuhiko Tomooka [c], Yutaka Watanabe [d], Sachio Morimoto [a], Yoshimichi Nakatsu [e], Teruhisa Tsuzuki [e], Yusaku Nakabeppu [f], Toshiyuki Sasaguri [a,*]

[a] *Department of Clinical Pharmacology, Faculty of Medical Sciences, Kyushu University, Fukuoka, Japan*
[b] *Global Medical Science Education Unit, Faculty of Medical Sciences, Kyushu University, 3-1-1 Maidashi, Higashi-ku, Fukuoka 812-8582, Japan*
[c] *Department of Molecular and Material Science, Institute for Materials Chemistry and Engineering, Kyushu University, Fukuoka, Japan*
[d] *Department of Applied Chemistry, Faculty of Engineering, Ehime University, Matsuyama, Japan*
[e] *Department of Medical Biophysics and Radiation Biology, Faculty of Medical Sciences, Kyushu University, Fukuoka, Japan*
[f] *Division of Neurofunctional Genomics, Department of Immunobiology and Neuroscience, Medical Institute of Bioregulation, Kyushu University, Fukuoka, Japan*

ARTICLE INFO

Article history:
Received 10 February 2014
Received in revised form 12 March 2014
Accepted 14 March 2014
Available online xxx

Keywords:
DIF-1
TCF7L2
GSK-3β
Wnt/β-catenin signaling pathway
Egr-1

ABSTRACT

We reported that differentiation-inducing factor-1 (DIF-1), synthesized by *Dictyostelium discoideum*, inhibited proliferation of various tumor cell lines *in vitro* by suppressing the Wnt/β-catenin signaling pathway. However, it remained unexplored whether DIF-1 also inhibits tumor growth *in vivo*. In the present study, therefore, we examined *in-vivo* effects of DIF-1 using three cancer models: *Mutyh*-deficient mice with oxidative stress-induced intestinal tumors and nude mice xenografted with the human colon cancer cell line HCT-116 and cervical cancer cell line HeLa. In exploration for an appropriate route of administration, we found that orally administered DIF-1 was absorbed through the digestive tract to elevate its blood concentration to levels enough to suppress tumor cell proliferation. Repeated oral administration of DIF-1 markedly reduced the number and size of intestinal tumors that developed in *Mutyh*-deficient mice, reducing the phosphorylation level of GSK-3β Ser^9 and the expression levels of early growth response-1 (Egr-1), transcription factor 7-like 2 (TCF7L2) and cyclin D1. DIF-1 also inhibited the growth of HCT-116- and HeLa-xenograft tumors together with decreasing phosphorylation level of GSK-3β Ser^9, although it was not statistically significant in HeLa-xenograft tumors. DIF-1 also suppressed the expressions of Egr-1, TCF7L2 and cyclin D1 in HCT-116-xenograft tumors and those of β-catenin, TCF7L2 and cyclin D1 in HeLa-xenograft tumors. This is the first report to show that DIF-1 inhibits tumor growth *in vivo*, consistent with its *in-vitro* action, suggesting that this compound may have potential as a novel anti-tumor agent.

1. Introduction

The Wnt/β-catenin signaling pathway, which is well conserved throughout biological evolution, regulates a number of cellular functions during embryonic development and in maintenance of tissue homeostasis by regulating somatic stem cells and their niches [1–3]. Accumulating evidence suggests that this pathway is often involved in oncogenesis and cancer development. Activation of the Wnt/β-catenin signaling pathway results in upregulation of its target genes, such as *CCND1* encoding cyclin D1 and *c-myc*, which play key roles in the initiation and progression of G_1 phase in the cell cycle [4,5], thereby promoting tumor formation [6–9]. In fact, this pathway is constitutively activated in most colorectal cancers, including those in patients with familial adenomatous polyposis (FAP), and other types of malignant tumors [10–14].

Glycogen synthase kinase-3β (GSK-3β) was first identified as a cytoplasmic serine/threonine protein kinase that phosphorylates glycogen synthase to inhibit its activity. However, it is now well known that this kinase plays central roles in various biological

* Corresponding authors at: Department of Clinical Pharmacology, Faculty of Medical Sciences, Kyushu University, 3-1-1 Maidashi, Higashi-ku, Fukuoka 812-8582, Japan. Tel.: +81 92 642 6887; fax: +81 92 642 6084.
E-mail addresses: yanaga@cliphrarm.med.kyushu-u.ac.jp (F. Takahashi-Yanaga), sasaguri@cliphrarm.med.kyushu-u.ac.jp (T. Sasaguri).

http://dx.doi.org/10.1016/j.bcp.2014.03.006
0006-2952/

processes including the Wnt/β-catenin signaling pathway [15,16]. GSK-3β inhibits the Wnt/β-catenin signaling pathway by phosphorylating β-catenin to accelerate its proteolysis [15,17], resulting in the inhibition of transcription of *CCND1*, *c-myc* and other Wnt target genes. In addition, GSK-3β phosphorylates cyclin D1 to promote its degradation. Accordingly, GSK-3β reduces cyclin D1 expression by two mechanisms: inhibition of *CCND1* gene transcription and promotion of cyclin D1 protein degradation [17,18]. Therefore, we thought the compounds that induce GSK-3β activation could be useful as anti-tumor agents.

We previously reported that differentiation-inducing factors (DIF-1 and DIF-3), which were identified in *Dictyostelium discoideum* as putative morphogens required for stalk cell differentiation [19,20], have a powerful antiproliferative effect on human cancer cell lines *in vitro* [21–27]. With regard to the underlying mechanisms, we revealed that DIFs accelerated degradation of cyclin D1 and β-catenin through the activation of GSK-3β, leading to the suppression of the Wnt/β-catenin signaling pathway and cell cycle arrest at the G_0/G_1 phase in various human cells [21–26]. Surprisingly, DIF-1 also suppressed proliferation of colon cancer cells in which the Wnt/β-catenin signaling pathway was constitutively activated by lack of β-catenin destruction mechanisms. In this regard, we revealed that DIF-1 suppressed transcription factor 7-like 2 (TCF7L2) expression via reduced early growth response-1 (Egr-1) protein amount, thereby inhibiting the Wnt/β-catenin signaling pathway without affecting β-catenin expression level [27]. However, the mechanisms for DIF-1's *in-vivo* action remain to be clarified.

Therefore, in the present study, to assess whether DIF-1 is applicable to the treatment of malignant tumors, we examined its *in-vivo* effects using mice. First, we examined its pharmacokinetics and toxicity. Second, we evaluated the anti-cancer effects of DIF-1 using a spontaneous cancer model and human cancer xenograft models. For the former, we employed *Mutyh*-deficient (*Mutyh*$^{-/-}$) mice, which lack the MutY homolog (MUTYH), a mammalian DNA glycosylase that initiates base excision repair, and is thus susceptible to oxidative stress-induced carcinogenesis [28–31]. These mice provide a useful animal model for examining colorectal adenoma and carcinoma [31]. For the latter, we used nude mice bearing HCT-116 cells and those bearing HeLa cells. Using these cancer models, we show for the first time that orally administered DIF-1 exhibits anti-tumor effects *in vivo*. Third, we examined the mechanisms for DIF-1's *in-vivo* actions.

2. Materials and methods

2.1. Chemicals and antibodies

DIF-1 (1-(3,5-dichloro-2, 6-dihydroxy-4-methoxyphenyl)-1-hexanone) was synthesized as described previously (purity: >98%) [32]. Celecoxib was kindly provided by Pfizer (New York, NY, USA). An anti-cyclin D1 polyclonal antibody was purchased from Santa Cruz Biotechnology (Santa Cruz, CA, USA). Anti-β-catenin and anti-GSK-3β monoclonal antibodies were purchased from R&D Systems (Minneapolis, MN, USA). Anti-Egr-1 monoclonal antibody, anti-transcription factor 7-like 2 (TCF7L2) monoclonal antibody (6H5-3) and anti-phospho-GSK-3β (Ser^9) polyclonal antibody were purchased from Cell Signaling Technology (Danvers, MA, USA). An anti-GAPDH monoclonal antibody was purchased from Abcam (Cambridge, MA, USA). An anti-α-tubulin monoclonal antibody was purchased from Calbiochem (Darmstadt, Germany). Growth factor-reduced Matrigel was obtained from BD Biosciences (San Jose, CA, USA).

2.2. Cell culture

HCT-116 and HeLa cells were grown in Dulbecco's modified Eagle's medium (Sigma, St. Louis, MO, USA) supplemented with 10% fetal bovine serum, 100 U/mL penicillin G, and 0.1 μg/mL streptomycin.

2.3. Western blot analysis

Protein samples (10 μg/lane) were separated by 12% SDS–polyacrylamide gel electrophoresis and then transferred to a polyvinylidene difluoride membrane using a semi-dry transfer system (1 h at 12 V). Western blot analysis was performed as described previously [21]. Optical densitometric scans were performed using NIH Image J software.

2.4. Administration of DIF-1

For intraperitoneal administration, 30 mg/kg DIF-1, pounded in a mortar and suspended in PBS, was injected into the abdomens of C57BL/6J male mice (10–11 weeks old; Kyudo, Tosu, Japan). For oral administration, DIF-1 was suspended in a 0.25% methylcellulose solution or dissolved in soybean oil. These DIF-1-containing solutions were then orally administered to the C57BL/6J mice.

2.5. Measurement of the DIF-1 concentration in mouse plasma

Mouse blood samples were collected by cardiac puncture at the indicated times, and plasma was isolated by centrifugation at 500 × *g* for 15 min. The plasma concentration of DIF-1 was determined by a reverse phase high-performance liquid chromatography (HPLC) system (Waters 2695, Milford, MA, USA) as described previously [33] with a slight modification. Briefly, mouse plasma samples (200 μL) containing 500 ng daisein (Wako Pure Chemical Industries Ltd., Osaka, Japan) as an internal standard were mixed with 200 μL chloroform. After mixing, the solution was centrifuged at 13,000 × *g* for 5 min, and then the organic phase was separated and evaporated. The residue was dissolved in 80 μL of a mixture of acetic acid (5%, v/v) and methanol (40%, v/v). A sample (50 μL) was then applied to a column for separation (TSKgel ODS-80Ts; Tosoh Corporation, Tokyo, Japan). The samples were eluted by a linear gradient of methanol (40–95%) in the presence of 5% acetic acid over 40 min at a flow rate of 1.0 mL/min. A UV detector was operated at 277 nm. A calibration curve was prepared by plotting the area ratios of DIF-1 normalized to the internal standard.

2.6. Intestinal tumor model mice

Intestinal tumors (adenomas and carcinomas) were formed by methods reported previously with slight modifications [31]. Briefly, $KBrO_3$ dissolved in drinking water at a concentration of 2 g/L was provided to 4-week-old mice for 12 weeks. At 16 weeks of age, the mice were randomly divided into six groups (six mice including three males and three females in each group). Mice in test groups were orally administered with DIF-1 or celecoxib, which was suspended in a 0.25% methylcellulose solution, once a day for 5 days/week over 4 weeks. Control mice received the vehicle only. The body weight of the mice was monitored weekly. At 20 weeks of age, all mice were sacrificed to obtain blood and intestinal samples. Blood samples were analyzed by a Celltac-alpha MEK-6358 (Nihon Kohden, Tokyo, Japan) for blood cell counts. Intestines were fixed in 4% formaldehyde, and the tumors were observed under a microscope. Images of the tumors were obtained and analyzed using NIH Image J software. For Western blot analysis, intestinal tissues (2 cm down from the pylorus) were homogenized in Laemmli's sample buffer immediately after

Please cite this article in press as: Takahashi-Yanaga F, et al. DIF-1 inhibits tumor growth *in vivo* reducing phosphorylation of GSK-3β and expressions of cyclin D1 and TCF7L2 in cancer model mice. Biochem Pharmacol (2014), http://dx.doi.org/10.1016/j.bcp.2014.03.006

resection. After adjustment of the protein content, the samples were electrophoresed and blotted with antibodies. Intestinal bleeding was examined in excrement by the guaiac reaction (Sionogi II test; Sionogi, Osaka, Japan).

2.7. Human cancer xenograft model mice

Eight-week-old female mice (BALB/c nu/nu) were subcutaneously injected in their right flank with 400 μL Matrigel and 5×10^6 human cancer cells (HCT-116 or HeLa) suspended in PBS (1:1, v:v). Mice were randomly divided into DIF-1 treatment and control groups. At the beginning, DIF-1 was suspended in a 0.25% methylcellulose solution and orally administered as in the experiment with intestinal tumor model mice. However, later, we improved the administration method to elevate plasma concentrations of DIF-1 by dissolving DIF-1 in soybean oil and dosing every 12 h (300 mg/kg in the morning and 150 mg/kg in the evening) for 5 days/week. Control group mice received the vehicles only. The body weight of mice was monitored weekly. Tumors removed on the indicated days were measured for size and weight, and then prepared for Western blot analysis. Blood samples were collected and analyzed for blood cell counts.

2.8. Statistical analysis

Results are expressed as the means ± s.e.m. Statistical analyses of differences between two mean values were performed using the Student's *t*-test. Multiple mean values were compared by one-way ANOVA with the Dunnett's multiple comparison test.

2.9. Ethics information

The study protocol was approved by the Committee of Ethics on Animal Experiments at Kyushu University (Permit Number: A22-046-0). Animal handling and procedures were carried out in compliance with the Guidelines for Animal Experiments, Kyushu University, and the Law (No. 105) and Notification (No. 6) of the Japanese Government. All surgeries were performed under sodium pentobarbital anesthesia, and all efforts were made to minimize suffering.

3. Results

3.1. Plasma concentration of DIF-1 in mice

To examine whether plasma DIF-1 concentrations reach levels that can show an antiproliferative effect on tumor cells, we measured DIF-1 concentrations after intraperitoneal and oral administration in wild-type C57BL/6J mice using a HPLC system. After intraperitoneal injection, the DIF-1 concentration rapidly increased and reached maximal levels (20–30 μg/mL) within 30 min, followed by a rapid decline (Fig. 1A). When orally administered, the DIF-1 concentration reached maximal levels (30–40 μg/mL) within 1 h, and the decline was much slower compared with that following intraperitoneal injection (Fig. 1B). Because the EC_{50} value of DIF-1 for an *in vitro* antiproliferative effect is 5–8 μg/mL, these results suggest that the plasma concentration of DIF-1 can be sufficiently elevated to show an

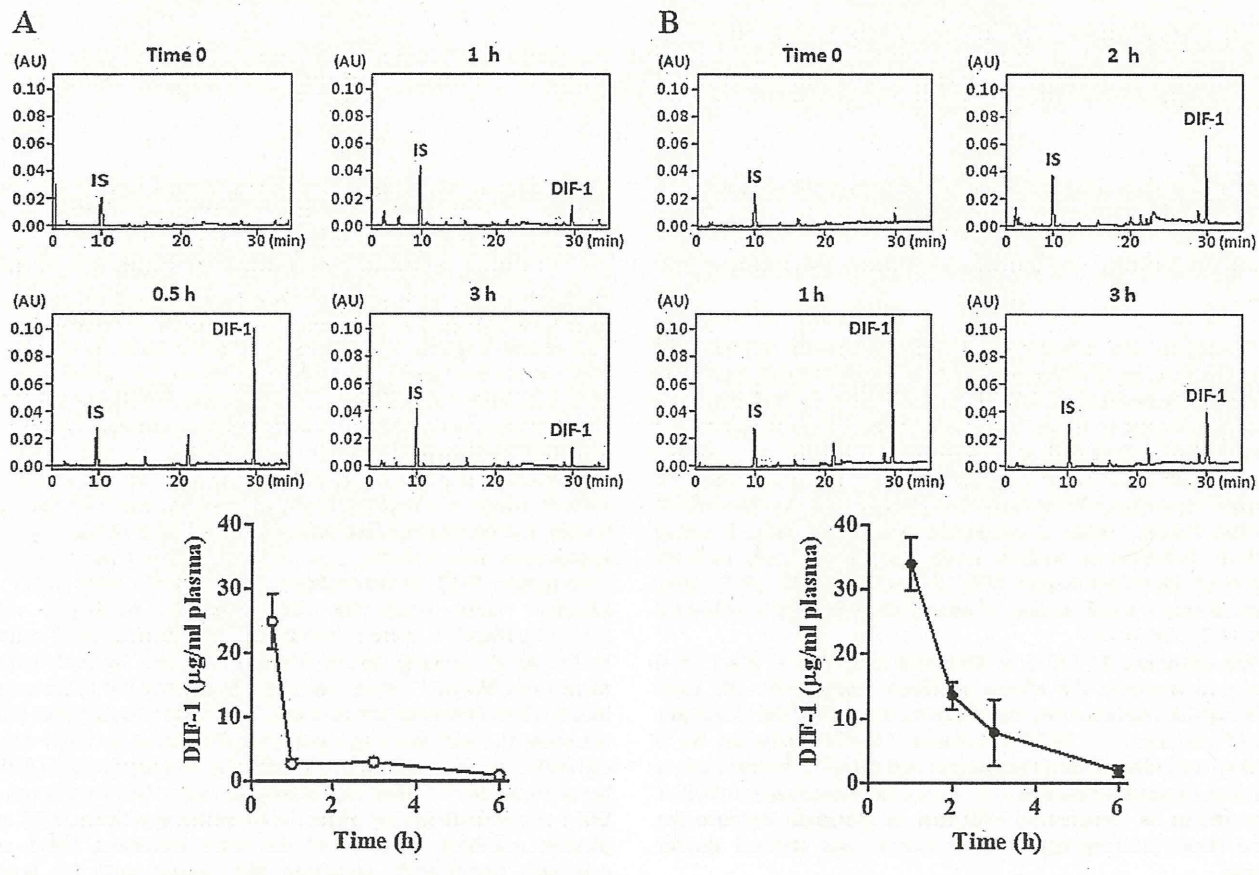

Fig. 1. Plasma concentrations of DIF-1.
DIF-1 was administered to mice intraperitoneally (A) or orally (B). Blood was collected at the indicated times to prepare HPLC samples. Upper panels: HPLC elution profiles. Lower panels: time course of plasma DIF-1 concentrations. Values are the means ± s.e.m. ($n = 3$). IS, internal standard.

Please cite this article in press as: Takahashi-Yanaga F, et al. DIF-1 inhibits tumor growth *in vivo* reducing phosphorylation of GSK-3β and expressions of cyclin D1 and TCF7L2 in cancer model mice. Biochem Pharmacol (2014), http://dx.doi.org/10.1016/j.bcp.2014.03.006